Structure and kinematic analysis of a novel 2-DOF translational parallel robot*

Chen Tao[1], Wu Chao[2] and Liu Xinjun[2]**

(1. School of Application Science and Technology, Harbin University of Science and Technology, Harbin 150080, China; 2. Department of Precision Instruments, Tsinghua University, Beijing 100084, China)

Accepted on February 13, 2007

Abstract This paper addresses the analysis of a novel parallel robot with 2 translational degrees of freedom (DOFs). The robot can position a rigid body in a plane with constant orientation. The kinematic structure of the robot is first described in detail. Some kinematic problems, such as the inverse and forward kinematics, velocity, and singularity are then analyzed. The working and assembly modes are discussed. Since it is the most important index to design a robot, the workspace of the robot is studied systematically in this paper. Based on the analysis of reachable workspace and singularity, a kind of workspace concept characterizing the region that the end-effector of the robot can reach in practice is defined. The results of this paper will be very useful for the design and application of the robot.

Keywords: parallel robot, degree of freedom, kinematics, workspace.

The conceptual design of parallel robots can be dated back to the time when Gough established the basic principles of a device with a closed-loop kinematic structure that can generate specified position and orientation of a moving platform so as to test tire wear and tear. Based on this principle, Stewart designed a platform used as an aircraft simulator in 1965[1]. In 1978, Hunt[2] made a systematic study of robots with parallel kinematics, in which the spatial 3-RPS (R-revolute joint, P-prismatic joint, and S-spherical joint) parallel robot is a typical one. Since then, parallel robots have been studied extensively by numerous researchers.

The parallel robots with 6 DOFs possess the advantages of high stiffness, low inertia, and large payload capacity. However, they suffer the problems of relatively small useful workspace and design difficulties[3]. Their direct kinematics possess a very difficult problem. The same problem of parallel robots with 2 and 3 DOFs can be described in a closed form[4]. As is well known, there are three kinds of singularities in parallel robots. Generally, not all singularities of a 6-DOF parallel robot can be found easily. For a parallel robot with 2 or 3 DOFs, the singularities can always be identified readily. For such reasons, parallel robots with less than 6 DOFs, especially 2 and 3 DOFs, have increasingly attracted more and more researchers' attention with respect to industrial applications[5—7]. In these designs, parallel robots with three translational DOFs have been playing important roles in the industrial applications. For example, the design of the DELTA robot is covered by a family of 36 patents[8]. Tsai's robot[5], in which each of the three legs consists of a parallelogram, is the first design to solve the problem of UU chain. Such parallel robots have wide applications in the industrial world, e.g., pick-and-place application, parallel kinematic machines, and medical devices.

The most famous planar 2-DOF parallel robots are the well-known five-bar mechanism with prismatic actuators or revolute actuators. In the case of the robot with revolute actuators, the mechanism consists of five revolute pairs and the two joints fixed to the base are actuated, while in the case of the robot with prismatic actuators, the mechanism consists of three revolute pairs and two prismatic joints, in which the prismatic joints are usually actuated. The output of the robot is the translational motion of a point on the end-effector. This means the orientation of the end-effector is also changed at any moment. Accordingly, some versions of the 2-DOF translational parallel robot (TPR) have been disclosed. One of them has

* Supported by National Natural Science Foundation of China (Grant No. 50505023) and High Technology Research and Development Program of China (Grant No. 2006AA04Z227)

** To whom correspondence should be addressed. E-mail: xinjunliu@mail.tsinghua.edu.cn

been applied in precise pick & place operations at high speed at SFB in Germany[9]. In 2001, another 2-DOF TPR has been proposed for the conceptual design of a 5-axis machine tool[4]. The structure, kinematics and dynamics of the TPR were discussed in detail[7]. Recently, a 2-DOF TPR with revolute actuators was introduced[10,11]. The TPR presented in Ref. [4] has been used in the design of a planer machine tool with a gantry structure instead of a traditional one with serial chains to improve its stiffness and inertia characteristics. However, all of these TPRs consist of at least of one parallelogram, which increases the difficulty of manufacturing and affects the accuracy.

This paper introduces a novel planar translational parallel robot with simple kinematic structure. The robot can position an objective with constant orientation. Some kinematic problems, such as inverse and forward kinematics, workspace and singularity are discussed.

1 Description of the 2-DOF TPR and its topological architectures

1.1 Architecture description

The novel 2-DOF translational parallel robot and its schematic are shown in Fig. 1. The end-effector of the robot is connected to the base by two kinematic legs 1 and 2. Leg 1 consists of three revolute joints and leg 2 two revolute joints and one cylinder joint, or three revolute joints and one prismatic joint. In each leg, the revolute joints are parallel to each other. The axes of the revolute joints in leg 1 are normal to those of the joints in leg 2. The two joints attached to the end-effector are put in the adjacent sides of a square. The kinematic chain of the robot is denoted as RRR-RRC (C-cylinder joint) or RRR-RRRP. One may see that, if the P joint is fixed, the robot is actually the famous Sarrus mechanism[12].

As introduced previously, other TPRs have at least one parallelogram in their structures. The TPR proposed here has no parallelogram. This makes the manufacturing easier. However, compared with the TPRs presented in Refs. [9, 10], the TPR studied here has some disadvantages. For example, the performance of the new TPR is not symmetric in its workspace. Additionally, the new TPR is likely to need more occupying space.

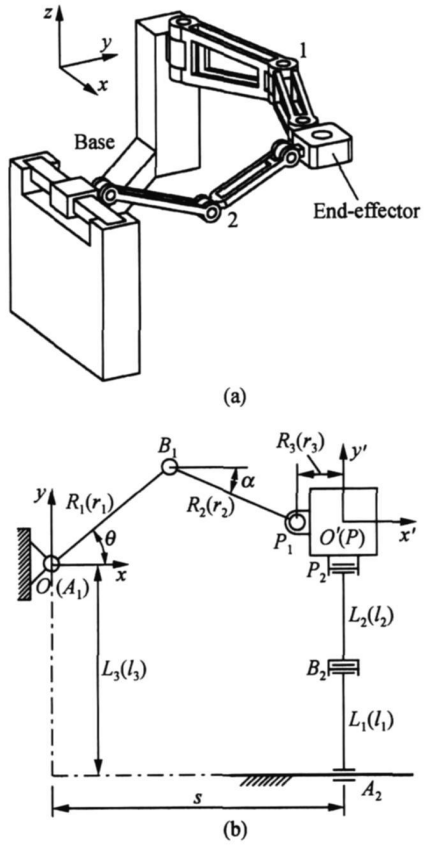

Fig. 1. The 2-DOF translational parallel robot. (a) the CAD model; (b) the schematic.

1.2 Capability

Here, an expression like $\aleph_j = (\bar{x}, \bar{y}, \bar{z}; \hat{x}, \hat{y}, \hat{z})$ is used to describe the capability of an object j. In $\aleph_j$, $Tr_j = (\bar{x}, \bar{y}, \bar{z})$ and $Ro_j = (\hat{x}, \hat{y}, \hat{z})$ express the translation and rotation of the object, respectively. If an element in $\aleph_j$ is equal to 0, there is no such a translation or rotation. If it is equal to 1, there is the capability. For example, $\bar{x} = 0$ means that the object has no translation along the x-axis; $\hat{y} = 1$ indicates that the object can rotate about the y-axis.

Observing only leg 1, the capability of the end-effector in the leg can be expressed as $\aleph_1 = (1, 1, 0; 0, 0, 1)$. Letting leg 1 alone, the capability of the end-effector with leg 2 can be written as $\aleph_2 = (1, 1, 1; 1, 0, 0)$. Then, the intersection of $\aleph_1$ and $\aleph_2$ is $\aleph$, i.e.,

$$\aleph = \aleph_1 \cap \aleph_1 = (1, 1, 0; 0, 0, 1) \cap (1, 1, 1; 1, 0, 0) = (1, 1, 0; 0, 0, 0) \quad (1)$$

which describes the capability of the robot, i.e., the translations of the end-effector along the x and y axes. This means the end-effector has two purely translational degrees of freedom with respect to the base.

It is noteworthy that the capability analysis method used above cannot be applied to all parallel robots.

2 Kinematics analysis

2.1 Inverse kinematics

As illustrated in Fig. 1(b), a reference frame $\Re$: O-xy is fixed to the base at the joint point A_1 and a moving reference frame $\Re'$: O'-$x'y'$ is attached to the end-effector, where O' is the reference point on the end-effector. Vectors $\boldsymbol{p}_{i\Re}(i=1,2)$ are defined as the position vectors of points P_i in the frame $\Re$ and vectors $\boldsymbol{b}_{i\Re}(i=1,2)$ as the position vectors of points B_i in frame $\Re$ The geometric parameters of the robot are $A_1B_1 = R_1(r_1)$, $B_1P_1 = R_2(r_2)$, $PP_i = R_3(r_3)$, $A_2B_2 = L_1(l_1)$, $B_2P_2 = L_2(l_2)$, and the distance from point A_1 to the guideway is $L_3(l_3)$, where R_n and $L_n(n=1,2,3)$ are dimensional parameters, and r_n and l_n non-dimensional parameters. The position of point O' in the fixed frame $\Re$ is denoted as vector

$$\boldsymbol{c}_{\Re} = (x, y)^{\mathrm{T}} \tag{2}$$

The vectors of $\boldsymbol{b}_{1\Re}$ in the fixed frame $\Re$ can be written as

$$\boldsymbol{b}_{1\Re} = (R_1\cos\theta, R_1\sin\theta)^{\mathrm{T}} \tag{3}$$

where θ is the actuated input for leg 1. Vector $\boldsymbol{p}_{1\Re}$ in the fixed frame $\Re$ can be written as

$$\boldsymbol{p}_{1\Re} = (-R_3, 0)^{\mathrm{T}} + \boldsymbol{c}_{\Re} = (x - R_3, y)^{\mathrm{T}} \tag{4}$$

The inverse kinematics problem of leg 1 can be solved by writing the following constraint equation

$$\| \boldsymbol{p}_{1\Re} - \boldsymbol{b}_{1\Re} \| = R_2 \tag{5}$$

that is

$$(x - R_3 - R_1\cos\theta)^2 + (y - R_1\sin\theta)^2 = R_2^2 \tag{6}$$

Then, there is

$$\theta = 2\tan^{-1}(m) \tag{7}$$

where

$$m = \frac{-b + \sigma\sqrt{b^2 - 4ac}}{2a} \tag{8}$$

$\sigma = 1$ or -1

$$a = (x - R_3)^2 + y^2 + R_1^2 - R_2^2 + 2(x - R_3)R_1$$

$$b = -4yR_1$$

$$c = (x - R_3)^2 + y^2 + R_1^2 - R_2^2 - 2(x - R_3)R_1$$

For leg 2, it is obvious that

$$s = x \tag{9}$$

in which s is the input of leg 2. From Eqs. (8) and (9), we can see that there are two solutions for the inverse kinematics of the robot. Hence, for a given robot and for prescribed values of the position of the end-effector, the required actuated inputs can be directly computed from Eqs. (7) and (9). To obtain the configuration as shown in Fig. 1, parameter σ in Eq. (8) should be 1. This configuration is called the "+" working mode. When $\sigma = -1$, the corresponding configuration is referred to as the "−" working mode.

2.2 Forward kinematics

The forward kinematic problem is to obtain the output with respect to a set of given inputs. From Eqs. (6) and (9), one obtains

$$y = e + \sigma\sqrt{f} \tag{11}$$

and

$$x = s \tag{12}$$

where $e = R_1\sin\theta$ and $f = R_2^2 - (s - R_3 - R_1\cos\theta)^2$. Therefore, there are also two forward kinematic solutions for the robot. The parameter $\sigma = -1$ corresponds to the configuration shown in Fig. 1, which is denoted as the down-configuration. When $\sigma = 1$, the configuration is referred to as the up-configuration. These two kinds of configurations correspond to two kinds of assembly modes of the robot.

3 Singularity analysis

3.1 Jocabian matrix

Equations (6) and (9) can be differentiated with respect to time to obtain the velocity equations. This leads to

$$\dot{s} = \dot{x} \tag{13}$$

$$R_1[y\cos\theta - (x - R_3)\sin\theta]\dot{\theta} = (x - R_3 - R_1\cos\theta)\dot{x} + (y - R_1\sin\theta)\dot{y} \tag{14}$$

which can be written in an equation of the form

$$\boldsymbol{A}\dot{\boldsymbol{q}} = \boldsymbol{B}\dot{\boldsymbol{p}} \tag{15}$$

where $\dot{\boldsymbol{q}} = (\dot{s} \quad \dot{\theta})^{\mathrm{T}}$ and $\dot{\boldsymbol{p}} = (\dot{x} \quad \dot{y})^{\mathrm{T}}$ are the joint and Cartesian space velocity vectors, respectively, and $\boldsymbol{A}$ and $\boldsymbol{B}$ are, respectively, the 2×2 matrices and can be expressed as

$$\boldsymbol{A} = \begin{bmatrix} 1 & 0 \\ 0 & R_1y\cos\theta - R_1(x - R_3)\sin\theta \end{bmatrix}$$

and

$$\boldsymbol{B} = \begin{bmatrix} 1 & 0 \\ x - R_3 - R_1\cos\theta & y - R_1\sin\theta \end{bmatrix} \tag{16}$$

If matrix $\boldsymbol{A}$ is nonsingular, the Jacobian matrix of the robot can be obtained as

$$\boldsymbol{J}=\boldsymbol{A}^{-1}\boldsymbol{B}=\begin{bmatrix}1 & 0\\ \dfrac{x-R_3-R_1\cos\theta}{R_1 y\cos\theta-R_1(x-R_3)\sin\theta} & \dfrac{y-R_1\sin\theta}{R_1 y\cos\theta-R_1(x-R_3)\sin\theta}\end{bmatrix} \tag{17}$$

from which one can see that there is no any parameter of L_n ($n=1, 2, 3$) in this matrix.

3.2 Singularity

In the parallel robot, singularities occur whenever $\boldsymbol{A}$, $\boldsymbol{B}$ or both, become singular. As a singularity leads to an instantaneous change of the robot's DOF, the analysis of parallel robots has drawn considerable attention. For the parallel robot studied here, since no parameter of leg 2 is involved in the Jacobian matrix (see Eqs. (16) and (17)), the singularity of the parallel robot is actually that of leg 1.

The stationary singularity occurs when $\boldsymbol{A}$ becomes singular but $\boldsymbol{B}$ remains invertible. $|\boldsymbol{A}|=0$ leads to $R_1 y\cos\theta-R_1(x-R_3)\sin\theta=0$, i.e., $\tan\theta=y/(x-R_3)$. This corresponds to the configuration when leg 1 $A_1B_1P_1$ is completely extended or folded. This singularity is also referred to as the serial singularity. For example, for the robot with the parameters $R_1=1.2$ mm and $R_2=0.8$ mm, two configurations of this kind of singularity are shown in Fig. 2. The loci of point P for this kind of singularity can be expressed as

$$C_{\text{fir\_o}}:\ (x-R_3)^2+y^2=(R_1+R_2)^2 \tag{18}$$

and

$$C_{\text{fir\_i}}:\ (x-R_3)^2+y^2=(R_1-R_2)^2 \tag{19}$$

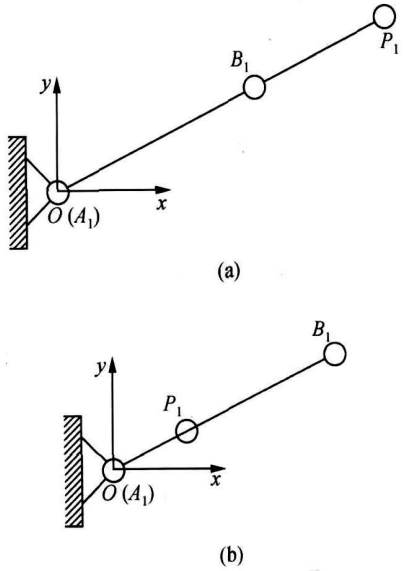

Fig. 2. Two kinds of configurations of the stationary singularity: (a) $A_1B_1P_1$ is completely extended; (b) $A_1B_1P_1$ is completely folded.

For the above example, if $R_3=0.5$ mm the loci of point P are shown in Fig. 3.

Note that $R_1=0$ leads to $\det(\boldsymbol{A})=0$ as well. Therefore, $R_1=0$ also results in this kind of singularity.

The uncertainty singularity, occurring only in closed kinematics chains, arises when $\boldsymbol{B}$ becomes singular but $\boldsymbol{A}$ remains invertible. $|\boldsymbol{B}|=0$ results in $y=R_1\sin\theta$. This corresponds to the configuration when link B_1P_1 is parallel to the x-axis. Two such configurations are shown in Fig. 4. In such a singularity, the loci of point P can be written as

$$C_{\text{sec\_r}}:\ (x-R_3-R_2)^2+y^2=R_1^2 \tag{20}$$

and

$$C_{\text{sec\_l}}:\ (x-R_3+R_2)^2+y^2=R_1^2 \tag{21}$$

It is noteworthy that the singular loci of a robot when R_1 is greater than R_2 are different from those when R_2 is greater than R_1. The two cases are shown in Fig. 3, from which we can see that the un-

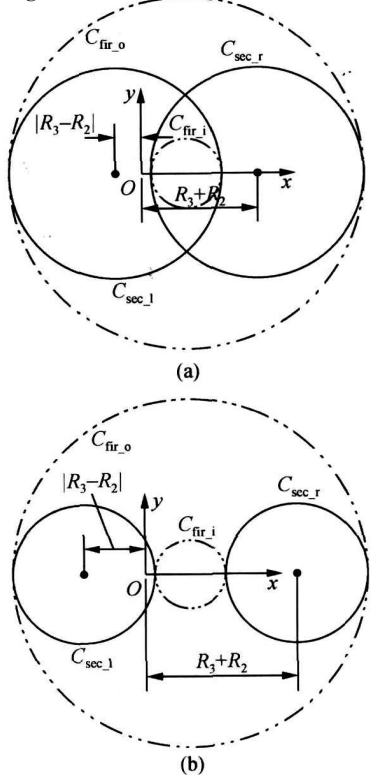

Fig. 3. Singular loci of point P when the robot is in the singularity. (a) $R_1\geqslant R_2$; (b) $R_1< R_2$. $C_{\text{fir\_o}}$ and $C_{\text{fir\_i}}$ are stationary singular loci; $C_{\text{sec\_r}}$ and $C_{\text{sec\_l}}$ are uncertainty singular loci.

certainty singular loci are always inside the region bounded by the stationary singular loci, and there are usually tangent points between the two kinds of loci.

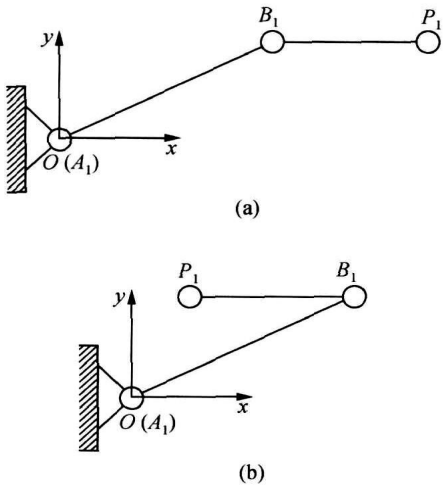

Fig. 4. Two kinds of configurations of the uncertainty singularity. (a) point P_1 is on the right of point B_1; (b) point P_1 is on the left of point B_1.

The analysis on the kinematics of the robot shows that there are two solutions for both the inverse and forward kinematics. Any one of the singularities will result in the change of solution number of the kinematics. For example, the stationary singularity leads to the loss of solution number of the inverse kinematics. In the uncertainty singular configuration, the solution number of the forward kinematics can be less or more than two. Then the stationary singularity can be called the inverse kinematic singularity, and the uncertainty singularity the forward kinematic singularity.

4 Workspace analysis

One of the most important issues in the design process of a robot is its workspace. For parallel robots, this issue may be more critical since parallel robots will sometimes have a rather limited workspace.

4.1 Theoretical workspace

Theoretical workspace of the studied robot is defined as the region that the output point can reach if θ changes from 0 to 2π and s between $-\infty$ and ∞ without the consideration of interference between links and singularity.

From Eq. (6), one can see that if θ is specified, the workspace of leg 1 is a circle centered at the point $(R_1\cos\theta+R_3, R_1\sin\theta)$ with a radius of R_2. The circle is denoted as C_{11}. If θ_i changes from 0 to 2π, the center point is located at a circle centered at point $(R_3, 0)$ with a radius of R_1. The circle is denoted as C_{12}. Then, the workspace of the leg is the enveloping region of circle C_{11} when its center rolls at circle C_{12}. Actually, the enveloping region is an annulus bounded by two circles $C_{\mathrm{fir\_o}}$ and $C_{\mathrm{fir\_i}}$ given in Eqs. (18) and (19), respectively. Especially, when $R_1=R_2$ the workspace is the region bounded by circle $C_{\mathrm{fir\_o}}$.

Thinking about the architecture of the studied parallel robot, we can see that the workspace of leg 1 is limited with respect to the parameters R_1 and R_2, while the workspace of leg 2 has the advantage along x-axis, which means the workspace can be infinite if the input s is not limited. Practically, this case cannot occur. However, to enlarge the workspace of the robot, we are sure to find a solution that the workspace of leg 1 can be embodied by that of leg 2. Actually, enlarging the workspace is our pursuing objective. In this sense, the workspace of the robot should be the workspace of leg 1, which is then our research objective.

For example, the theoretical workspace of leg 1 of the robot with parameters $R_1=1.2$ mm, $R_2=0.8$ mm and $R_3=0.5$ mm is shown as the shaded region in Fig. 5. The theoretical workspace and any other type of workspace of the robot can be that which embodies the corresponding workspace of leg 1 by assigning appropriate values to the parameters L_n ($n=1, 2, 3$). Therefore, in this chapter, the workspace of leg 1 is regarded as the workspace of the parallel robot.

The theoretical workspace is actually bounded by the stationary singularity loci $C_{\mathrm{fir\_i}}$ and $C_{\mathrm{fir\_o}}$. Its area can be calculated by

$$S_{\mathrm{tw}}=\pi[(R_1+R_2)^2-(R_1-R_2)^2]=4\pi R_1R_2 \tag{22}$$

From Fig. 3, we can see that within the theoretical workspace there is stationary singularity.

4.2 Usable workspace

As there exist singular loci inside the theoretical workspace, when a robot wants to move from one point to another, it maybe passes a singular configu-

ration. It means that it should change from one working mode to another. In practice, changing working mode during the working process is definitely impossible. Therefore, we should find out a working space without singularity.

The usable workspace is defined as the maximum continuous workspace that contains no singular loci inside but bounded by singular loci outside. According to this definition, not every point within the usable workspace can be available for a practical robot. The robot will be out of control at the points on the boundaries and their neighborhoods. But within this region, the robot with a specified working mode can move freely.

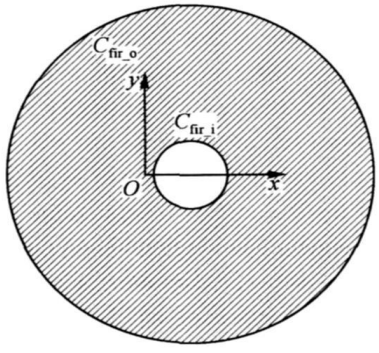

Fig. 5. Theoretical workspace of the robot.

In Section 3.2, two kinds of singular loci have been presented for the robot as shown in Fig. 6. The stationary singularity is actually the boundary of a theoretical workspace. Then, a robot with every working mode can have such singular loci. However, as the uncertainty singularity occurs inside the workspace, not every working mode has all such singularities. Normally, for most parallel robots studied here, there are four tangent points between the two kinds of singular loci. The points can be used to identify which singular loci a specified working mode can have. For example, all singular loci of the robot R_1 = 1.2 mm, R_2 = 0.8 mm and R_3 = 0.5 mm are shown in Fig. 3. Fig. 6 shows some singular configurations and singular loci of the robot. As shown in Fig. 6, there are four tangent points m, v, q and k between the four singular loci C_{fir_i}, C_{fir_o}, C_{sec_l} and C_{sec_r}. At these four points, both of the stationary and uncertainty singularities occur. The four points divide the singular curves C_{sec_l} and C_{sec_r} into four parts. At the arcs $m1q$ and $v3k$, the robot is in singular only when it is with the "+" mode. At the arcs $m2q$ and $v4k$, the working mode "−" is in singular.

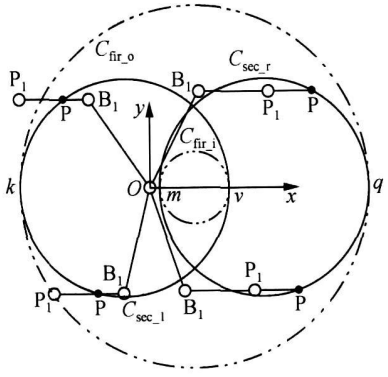

Fig. 6. The uncertainty singular loci of a robot with different working modes.

What we are concerned about here is the robot with the "+" working mode. Fig. 7 shows all singular loci of such kinds of robots.

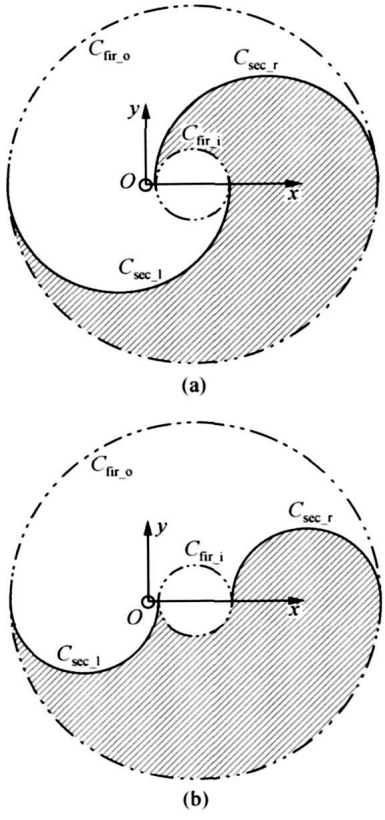

Fig. 7. Singular loci and usable workspace of the robot with both the "+" working mode and down-configuration. (a) $R_1 \geqslant R_2$; (b) $R_1 < R_2$.

The theoretical workspace is divided into two parts by the singular loci shown in Fig. 7, which can be used to identify the usable workspaces of the robots with the "+" working mode and, at the same time,

the down-configuration. In order to reduce the occupying space, the lower region shown in Fig. 7 is referred to as the usable workspace of the parallel robot. They are shown as the shaded region in Fig. 7. Actually, the usable workspace is half of the theoretical workspace. The area can be calculated by

$$S_{uw} = \frac{\pi}{2}[(R_1 + R_2)^2 - (R_1 - R_2)^2] = 2\pi R_1 R_2 \tag{23}$$

4.3 Good-condition workspace

As is well known, the local conditioning index (LCI) is defined as the reciprocal of condition number of the Jacobian matrix. Let's first check how the LCI is at every point in the workspace of the similarity robot with parameters $R_1 = 1.2$ mm, $R_2 = 0.8$ mm and $R_3 = 0.5$ mm. Its usable workspace is shown in Fig. 7(a). Fig. 8 shows the distribution of the LCI in the workspace.

From Fig. 8 one can see that, in the usable workspace, there exist some points where the LCI will be zero or very small. At these points the control accuracy of the robot will be very poor. These points will not be used in practice and should be excluded in the design process. The left workspace, which will be used in practice, can be referred to as good-condition workspace (GCW) that is bounded by a specified LCI value, i.e., $1/\kappa$. Then, the set of points where the LCI is greater than or equal to (GE) a specified LCI is defined as the GCW. For example, letting the LCI be specified as 0.36, the GCW of the robot with parameters $R_1 = 1.2$ mm, $R_2 = 0.8$ mm and $R_3 = 0.5$ mm will be the region enclosed by the curve with 0.36 as shown in Fig. 8.

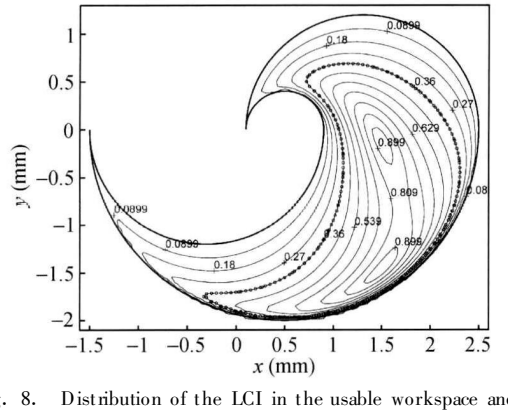

Fig. 8. Distribution of the LCI in the usable workspace and the good-condition workspace.

5 Conclusion and future work

In this paper, a novel 2-DOF translational robot is proposed. One characteristic of the robot is that it can position a rigid body in a 2D plane while maintaining a constant orientation. The proposed robot has potential application in light industry. The inverse and forward kinematics problems, workspace, and singularity are presented here.

The future work will focus on the kinematic design based on the workspace concept, the development of the computer-aided design of the robot based on the proposed design methodology, the development of the robot prototype, and the experience research of the prototype.

References

1 Stewart D. A platform with six degrees of freedom. Proceedings of the Institution of Mechanical Engineers, 1965(180): 371—386
2 Hunt KH. Structural kinematics of in-parallel-actuated robotarms. ASME Journal of Mechanism, Transmission and Automation in Design, 1983, 105: 705—712
3 Merlet JP. Parallel Robots. London: Kluwer Academic Publishers, 2000
4 Liu XJ. Mechanical and kinematics design of parallel robotic mechanisms with less than six degrees of freedom. Post-Doctoral Research Report (in Chinese), Tsinghua University, Beijing, 2001
5 Tsai LW and Stamper R. A parallel manipulator with only translational degrees of freedom. In: Proceedings of ASME 1996 Design Engineering Technical Conference, Irvine, CA, 1996, paper 96-DETC-MECH-1152
6 Siciliano B. The tricept robot: inverse kinematics, manipulability analysis and closed- loop direct kinematics algorithm. Robotica, 1999, 17: 437—445
7 Liu XJ, Wang QM and Wang J. Kinematics, dynamics and dimensional synthesis of a novel 2-DoF translational manipulator. Journal of Intelligent & Robotic Systems, 2005, 41: 205—224
8 Clavel R. DELTA: a fast robot with parallel geometry. In: Proceedings of 18th Int. Symp. on Industrial Robot, Sydney, 1988, 91—100
9 Collaborative Research Centers (SFB), SFB 562- Robotic systems for handling and assembly: Seitentitel: PORTYS, http://www.tu-braunschweig.de/sfb562/galerie/portys, 2007-2-13
10 Liu XJ and Wang J. Some new parallel mechanisms containing the planar four-bar parallelogram. International Journal of Robotics Research, 2003, 22: 717—732
11 Huang T, Li Z, Li M, et al. Conceptual design and dimensional synthesis of a novel 2-DOF translational parallel robot for pick-and-place operations. Journal of Mechanical Design, 2004, 126: 449—455
12 Sarrus PT. Note sur la Transformation des Mouvements Rctilignes Alternatifs, en Mouvements Circulairs, et Reciproquement. Comptes Rendus Hebdomadaires des Seances de l'Academie des Sciences, 1853, 36: 1036—1038